Methods

Expression and purification of the GORK proteins

The genes of *Arabidopsis* full-length *At*GORK (AT5G37500) and truncated variants (*At*GORK^{623}, residues 1-623 and *At*GORK^{510}, residues 1-510) were cloned into a modified pEG BacMam vector, which included a PreScission protease cleavage site, GFP, an 8× His tag, twin-Strep tag, and Flag tag at the N-terminus. Recombinant proteins were expressed in HEK293F cells. In short, baculovirus was generated in *Sf9* insect cells, and P2 viruses were used to infect HEK293F cells. Cells were cultured in suspension, supplemented with 1% (v/v) fetal bovine serum, and maintained at 37 °C with 70% humidity and 6% CO_2. Cells were infected with P2 viruses at a density of approximately 2.6×10^6 cells/mL, and supplemented with 10 mM sodium butyrate upon 8 hours post-infection, and continued to grow at 30℃ for another 50 hours. Cells were harvested, centrifuged, and stored at -80°C.

Harvested cells from 300 mL of culture were resuspended in extraction buffer (20 mM HEPES-Na pH 8.0, 150 mM KCl, 10 mM DDM, 2 mM cholesteryl hemisuccinate (CHS) supplemented with protease inhibitors (2 μg/mL pepstatin, 2 μg/mL aprotinin, 2 μg/mL leupeptin and 1 mM phenylmethylsulfonyl fluoride) and incubated at 4℃ for 2 hours. Solubilized membranes were clarified by centrifugation at 41,000 rpm for 1 hour, and the supernatant was loaded onto a Streptactin Beads 4FF column. Following a 5-column volume buffer wash, proteins were eluted with solubilization buffer (20 mM HEPES-Na pH 8.0, 150 mM KCl, 0.02% GDN, and 2.5 mM desthiobiotin). After tag removal with TEV protease, the proteins were further purified using a Superose-6 column in solubilization buffer (20 mM HEPES-Na pH 8.0, 150 mM KCl, 0.006% GDN). The elution was analyzed by SDS-PAGE, and the peak fractions of the purified protein were pooled and concentrated to ~3.5 mg/mL.

For the preparation of truncated truncated versions (*At*GORK^{623} and *At*GORK^{510}), we followed similar procedures as above.

Cryo-EM grid preparation and data acquisition

The protein sample (4 µl, ~3.5 mg/ml) was applied to freshly glow-discharged holy carbon film grids (Quantifoil, Cu, R1.2/1.3, 300 mesh) and blotted for 6.5 seconds at 100% humidity and 4°C using a Vitrobot Mark IV (Thermo Fisher Scientific), followed by plunge freezing into liquid ethane.

All the films were collected on a Titan Krios transmission electron microscope (Thermo Fisher Scientific, USA) operated at 300 kV equipped with a Gatan K2 or K3 Summit direct detection camera (Gatan Company, USA). Movies were recorded at 22,500× (for K3, corresponding 1.06 Å per pixel) or 130,000 × (for K2 summit, corresponding 1.04 Å per pixel) nominal magnifications, using SerialEM software with a beam-image shift method (Mastronarde, 2005; Wu et al., 2019), at a total dose of 50 e-/Å2 distributed over 32 frames, with defocus values between -1.2 and -2.2 µm.

Data processing and model building

All image processing steps were conducted using either CryoSPARC 3.1 (Punjani et al., 2017) or RELION 3.0 (Zivanov et al., 2018). CryoSPARC 3.1 was primarily used for reconstruction, while RELION 3.0 was employed for alignment-free 3D classification to identify an alternate conformation (*At*GORK^{FL2}) of the wild-type structure. Angular information was converted using PyEM, and map analysis and adjustments were performed with UCSF Chimera (Pettersen et al., 2004).

Raw movie frames were aligned using a dose-weighted patch alignment method, followed by CTF estimation. Particle picking was performed an oval template (88 × 168 Å), and coordinates were screened using normalized cross-correlation and local power scores to eliminate false positives. Particles were then down-sampled to a quarter size and classified based on shape (circular for top-view projections and T-shaped for side-view projections) after initial 2D classification to improve classification efficacy. A preliminary 3D reconstruction was generated from a small subset of particles.

*At*GORK^{FL1} was constructed with Nu-refinement using C2 symmetry with 156,313 particles, while *At*GORK^{FL2} used 39,551 particles with C1 symmetry. The resolutions were 3.4 Å for *At*GORK^{FL1} and 4.3 Å for *At*GORK^{FL2}, respectively. The alphafold2-predicted *Arabidopsis* GORK structure was used as the initial model, fitted

by individual domains in UCSF ChimeraX (Pettersen et al., 2021), and refined iteratively in Coot (Emsley et al., 2010) and PHENIX (Liebschner et al., 2019), and corrected iteratively. For the truncated *At*GORK^{623} and *At*GORK^{510}, the TMD structure from *At*GORK^{FL1} was used as the initial model, followed by iterative refinement and iterative adjustments in Coot and PHENIX. The resolutions were 3.2 Å for *At*GORK^{623} and 3.4 Å for *At*GORK^{510}, respectively. All figures were generated using UCSF ChimeraX.

Electrophysiology

The electrophysiological experiments were performed as previously described (Deng et al., 2021). Briefly, untagged coding sequences of *At*GORK wild type or mutated variants were cloned into the pGHME2 vector for expression in *Xenopus* oocytes. cRNAs were synthesized using T7 polymerase with linearized plasmid DNA templates. Oocyte sacs were extracted and digested with 0.2 mg/ml collagenase (Sigma) in OR2 buffer (82.5 mM NaCl, 2.5 mM KCl, 1 mM $MgCl_2$, and 5 mM HEPES-Na pH 7.5). For expression, 36 ng of wild-type GORK cRNA was injected per oocyte, with mutant cRNA doses adjusted to equimolar concentrations. Injected oocytes were incubated at 18°C in ND96 buffer (96 mM NaCl, 1.8 mM $CaCl_2$, 1 mM $MgCl_2$, 2 mM KCl, and 5 mM HEPES-Na pH 7.5) for 48 hours before use.

TEVC recordings were performed using an OC-725C amplifier (Warner Instruments) and Digidata 1550B (Molecular Devices) controlled by pClamp software. The bath solution contained (in mM): 10 KCl, 90 NaCl, 1 $CaCl_2$, 2 $MgCl_2$, and 10 Tris/MES (pH 7.4), with osmolarity adjusted to ~220 mOsmol/kg using D-mannitol. Microelectrodes (0.5-1 MΩ resistance) were filled with 3 M KCl, and agar bridges served as bath electrodes. Voltage steps from -110 mV to +70 mV (20-mV increments, 2,000 ms duration) were applied, followed by -110 mV clamping for 450 ms, 4,000 ms, or 16,000 ms depending on deactivation kinetics. Steady-state currents were measured at 50 ms before the end of each step. Data were analyzed using Clampfit 10.6 (Molecular Devices), Prism 8.0 (GraphPad), and Origin 2021.

Fluorescence and confocal imaging

To assess the cell-surface expression of full-length and C-terminal truncated GORK channels in *Xenopus* oocytes, GFP was fused to the N-terminus of each construct. The corresponding cRNAs were injected into oocytes, which were then incubated at 18°C for ~48 hours in ND96 buffer (detailed in the *Electrophysiology* section). GFP-tagged protein expression was verified using a confocal laser scanning microscope (Zeiss LSM 980), and fluorescence intensities were quantified with ImageJ. To minimize variability in expression levels due to experimental factors (e.g., cRNA injection dose or incubation time), all experiments were performed in parallel.

Data availability: All data generated or analysed in this paper are presented in the main text, figures and the extended data figures and supplementary videos, or are available from the corresponding author upon request. The cryo-EM maps of the *At*GORK full-length (*At*GORK^{FL1} and *At*GORK^{FL2}) and truncated version (*At*GORK^{623} and *At*GORK^{510}) have been deposited in the Electron Microscopy Data Bank with accession codes EMD-62338, EMD-37500, EMD-62337 and EMD-62339, respectively, and their structural models have been deposited in the PDB with accession codes 9KHF, 8WFZ, 9KHE and 9KHG, respectively (Supplementary Table S1).

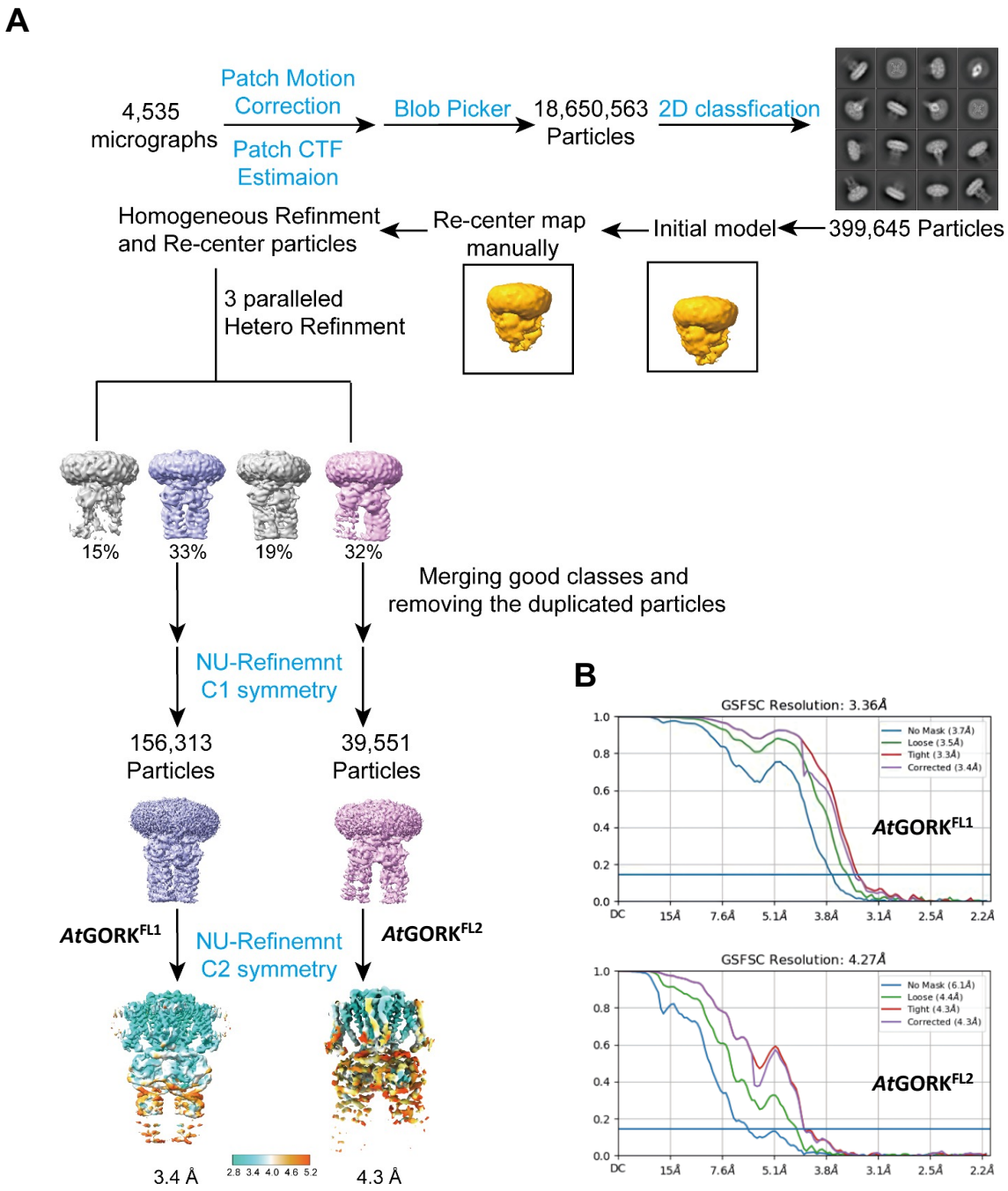
A
4,535 micrographs
Patch Motion Correction
Patch CTF Estimaion
Blob Picker
18,650,563 Particles
2D classfication
399,645 Particles
Initial model
Re-center map manually
Homogeneous Refinment and Re-center particles
3 paralleled Hetero Refinment
15%
33%
19%
32%
Merging good classes and removing the duplicated particles
NU-Refinemnt C1 symmetry
156,313 Particles
39,551 Particles
AtGORKFL1
AtGORKFL2
NU-Refinemnt C2 symmetry
3.4 Å
4.3 Å
B
GSFSC Resolution: 3.36Å
No Mask (3.7Å)
Loose (3.5Å)
Tight (3.3Å)
Corrected (3.4Å)
AtGORKFL1
GSFSC Resolution: 4.27Å
No Mask (6.1Å)
Loose (4.4Å)
Tight (4.3Å)
Corrected (4.3Å)
AtGORKFL2
C
S1
S2
S3
S4
S5
Pore helix
S6

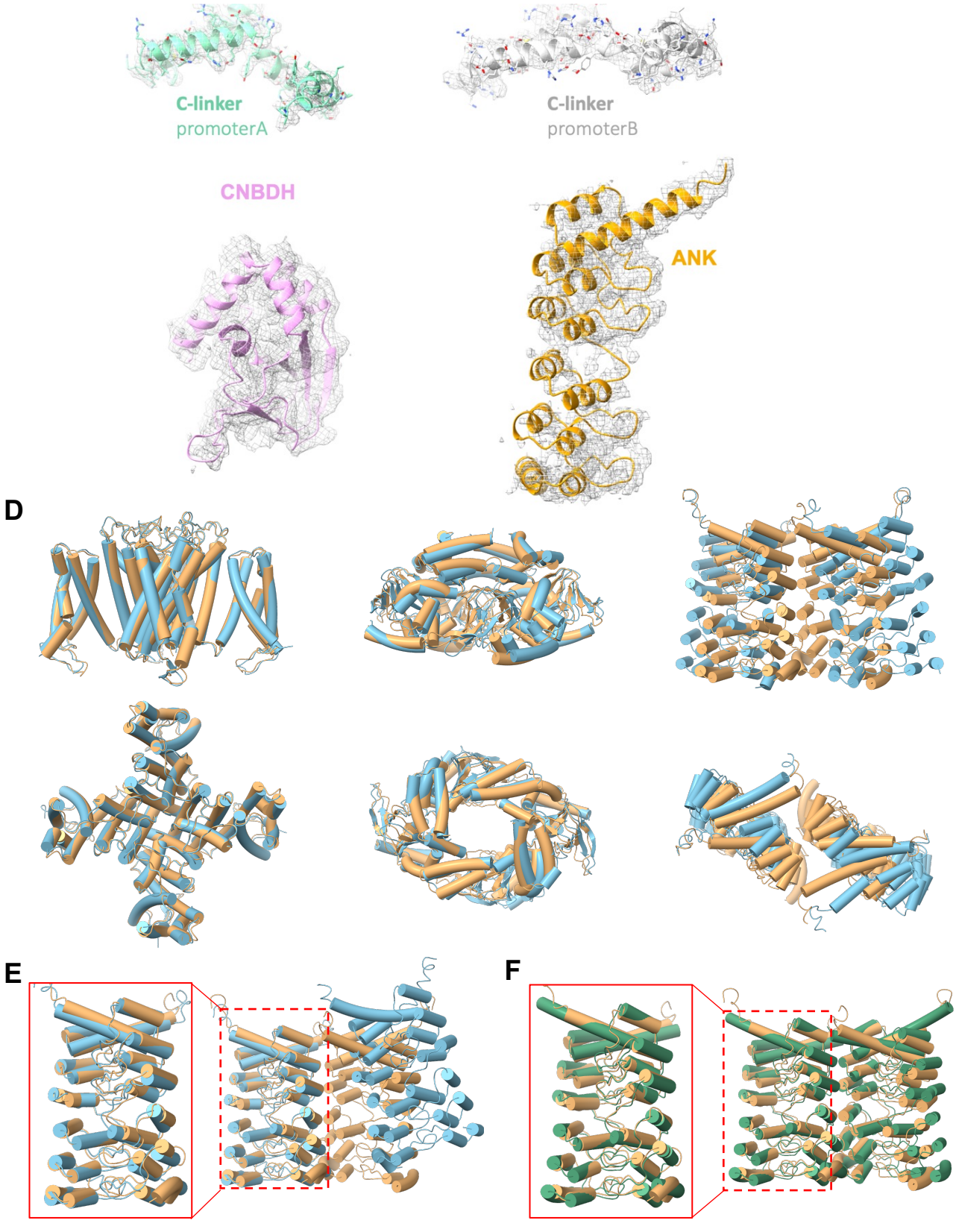

Figure S1. Structural determination of full-length *Arabidopsis* GORK (*At*GORK^{FL}).

(**A**) Workflow for image processing of full-length *Arabidopsis* GORK. (**B**) Fourier shell correlation (FSC) curve indicating overall resolution of 3.4 Å for *At*GORK^{FL1} and 4.3 Å for *At*GORK^{FL2}, as estimated using the 0.143 cut-off criterion (dotted line). (**C**) Representative cryo-EM density map showing TM segments (S1-S6) and domains (C-linker, CNBDH and ANK). (**D**) Structural comparison of domains in *At*GORK^{FL1} (light orange) and *At*GORK^{FL2} (light blue). (**E**) Superimposition of ANK dimers in *At*GORK^{FL1} (light orange) and *At*GORK^{FL2} (light blue), with a RMSD of 1.21 Å/dimer. (**F**) Superimposition of ANK dimers in *At*GORK^{FL1} (light orange) and *At*SKORK (purple, 8jet), with a RMSD of 1.33 Å/dimer. Despite variations in ANK conformation across the tetramer, the dimeric interaction is conserved, indicating that ANK dimerization is a fundamental structural feature of potassium channels with ANK domains.

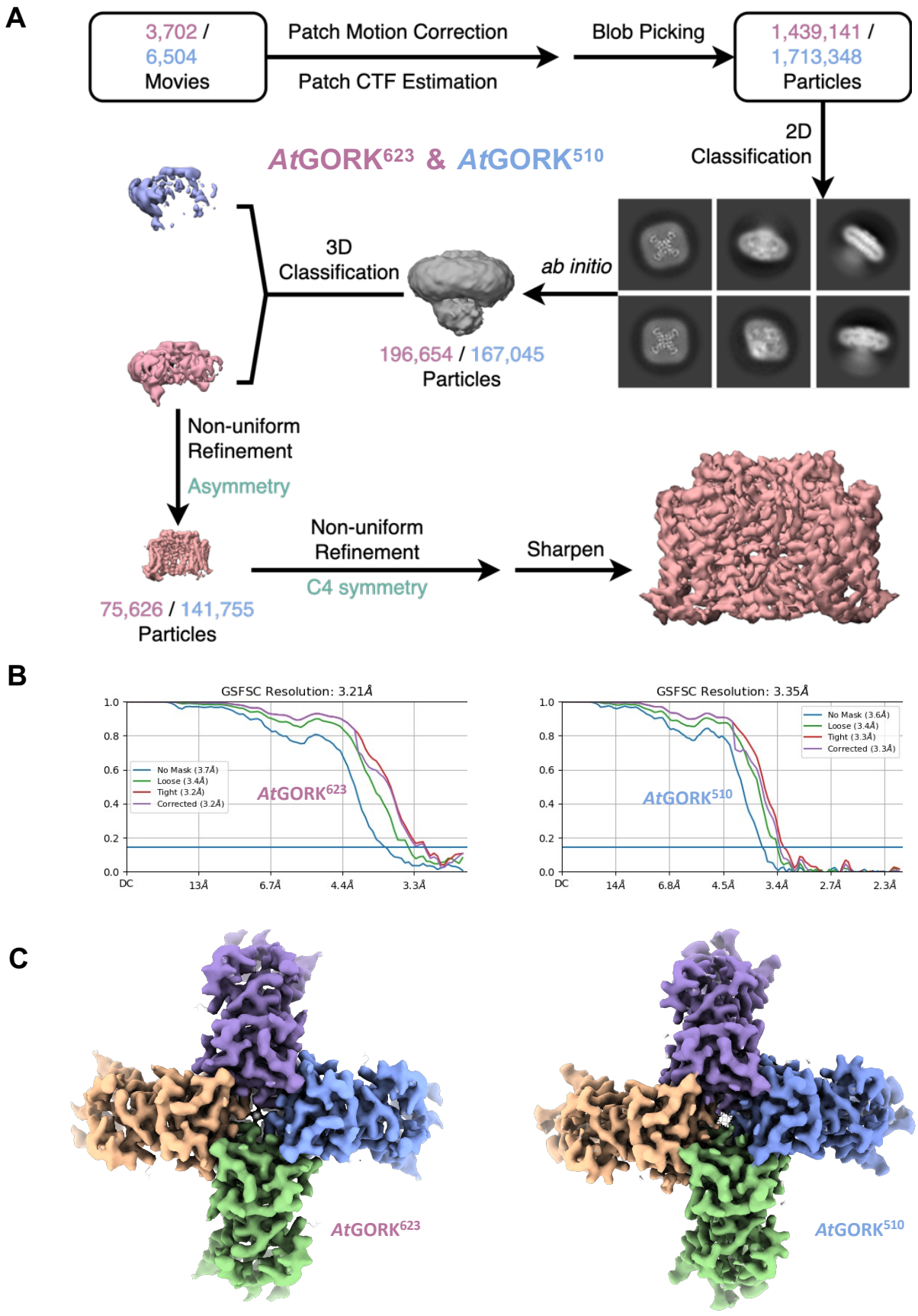

Figure S2. Structural determination of the truncated *At*GORK^{623} and *At*GORK^{510}.

(**A**) Workflow for image processing of the truncated *At*GORK^{623} (residues 1-623) and *At*GORK^{510} (residues 1-510). (**B**) Fourier shell correlation (FSC) curve indicating overall resolution of 3.2 Å for *At*GORK^{623} and 3.4 Å for *At*GORK^{510}, as estimated using the 0.143 cut-off criterion (dotted line). (**C**) Cryo-EM structures of *At*GORK^{623} (3.2 Å, left) and *At*GORK^{510} (3.4 Å, right).

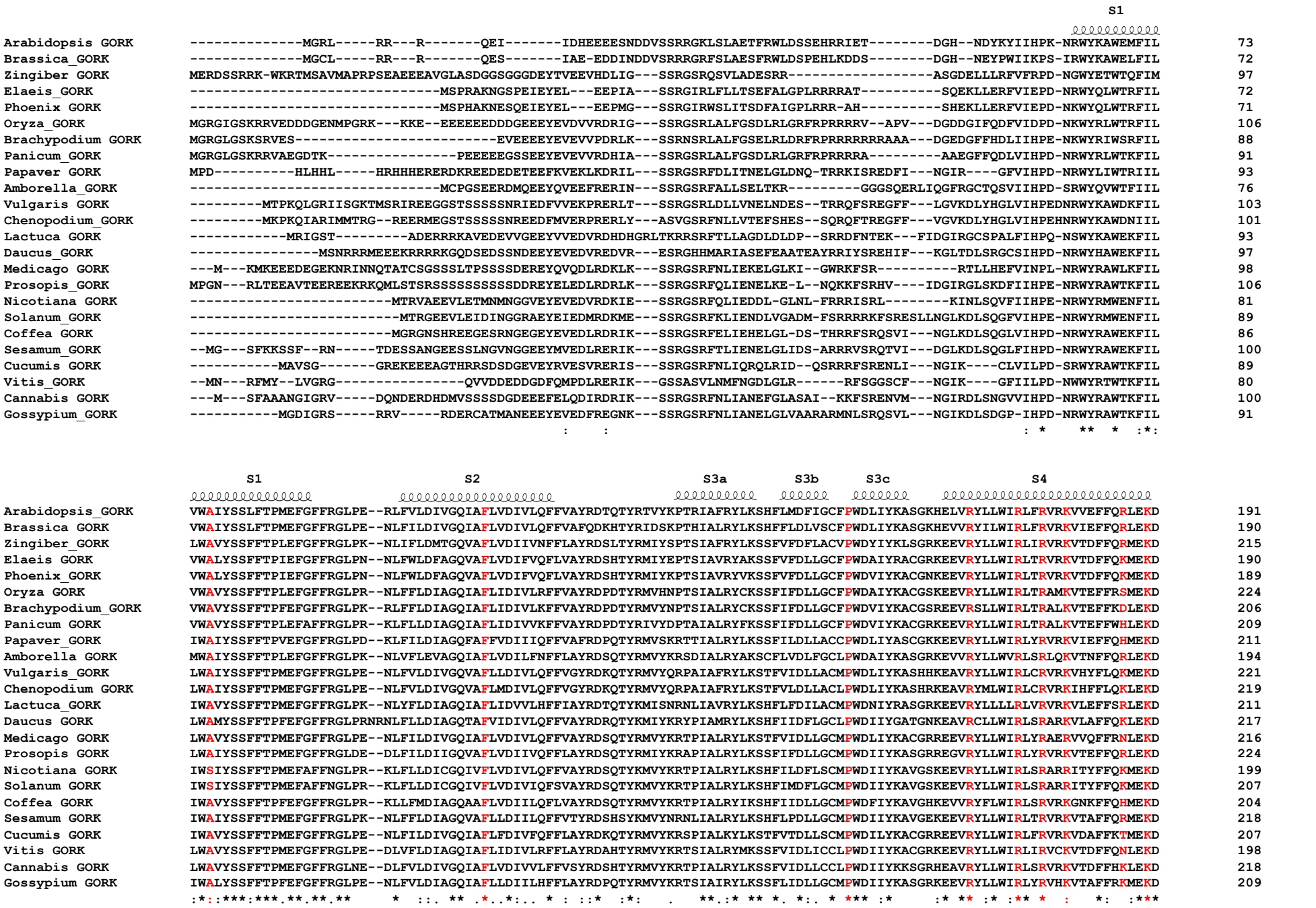
S1
Arabidopsis_GORK
Brassica_GORK
Zingiber_GORK
Elaeis_GORK
Phoenix_GORK
Oryza_GORK
Brachypodium_GORK
Panicum_GORK
Papaver_GORK
Amborella_GORK
Vulgaris_GORK
Chenopodium_GORK
Lactuca_GORK
Daucus_GORK
Medicago_GORK
Prosopis_GORK
Nicotiana_GORK
Solanum_GORK
Coffea_GORK
Sesamum_GORK
Cucumis_GORK
Vitis_GORK
Cannabis_GORK
Gossypium_GORK
S1
S2
S3a
S3b
S3c
S4
Arabidopsis_GORK
Brassica_GORK
Zingiber_GORK
Elaeis_GORK
Phoenix_GORK
Oryza_GORK
Brachypodium_GORK
Panicum_GORK
Papaver_GORK
Amborella_GORK
Vulgaris_GORK
Chenopodium_GORK
Lactuca_GORK
Daucus_GORK
Medicago_GORK
Prosopis_GORK
Nicotiana_GORK
Solanum_GORK
Coffea_GORK
Sesamum_GORK
Cucumis_GORK
Vitis_GORK
Cannabis_GORK
Gossypium_GORK

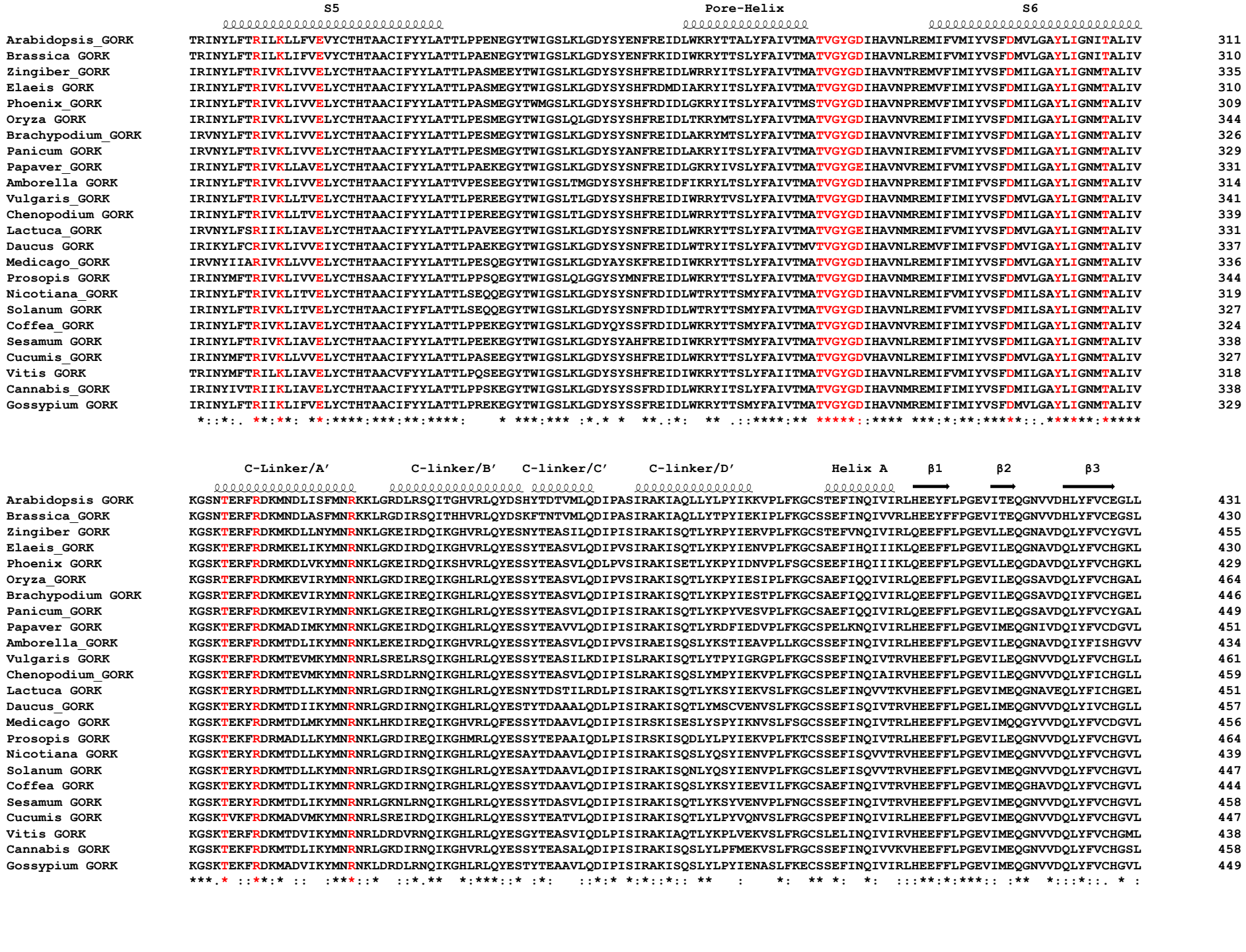
S5
Pore-Helix
S6
Arabidopsis_GORK TRINYLFTRILKLLFVEVYCTHTAACIFYYLATTLPPENEGYTWIGSLKLGDYSYENFREIDLWKRYTTALYFAIVTMATVGYGDIHAVNLREMIFVMIYVSFDMVLGAYLIGNITALIV 311
Brassica_GORK TRINYLFTRILKLIFVEVYCTHTAACIFYYLATTLPAENEGYTWIGSLKLGDYSYENFRKIDIWKRYTTSLYFAIVTMATVGYGDIHAVNLREMIFVMIYVSFDMVLGAYLIGNITALIV 310
Zingiber_GORK IRINYLFTRIVKLIVVELYCTHTAACIFYYLATTLPASMEEYTWIGSLKLGDYSYSHFREIDLWRRYITSLYFAIVTMATVGYGDIHAVNTREMVFIMIYVSFDMILGAYLIGNMTALIV 335
Elaeis_GORK IRINYLFTRIVKLIVVELYCTHTAACIFYYLATTLPASMEGYTWIGSLKLGDYSYSHFRDMDIAKRYITSLYFAIVTMATVGYGDIHAVNPREMVFIMIYVSFDMILGAYLIGNMTALIV 310
Phoenix_GORK IRINYLFTRIVKLIVVELYCTHTAACIFYYLATTLPASMEGYTWMGSLKLGDYSYSHFRDIDLGKRYITSLYFAIVTMSTVGYGDIHAVNPREMVFIMIYVSFDMILGAYLIGNMTALIV 309
Oryza_GORK IRINYLFTRIVKLIVVELYCTHTAACIFYYLATTLPESMEGYTWIGSLQLGDYSYSHFREIDLTKRYMTSLYFAIVTMATVGYGDIHAVNVREMIFIMIYVSFDMILGAYLIGNMTALIV 344
Brachypodium_GORK IRVNYLFTRIVKLIVVELYCTHTAACIFYYLATTLPESMEGYTWIGSLKLGDYSYSNFREIDLAKRYMTSLYFAIVTMATVGYGDIHAVNVREMIFIMIYVSFDMILGAYLIGNMTALIV 326
Panicum_GORK IRVNYLFTRIVKLIVVELYCTHTAACIFYYLATTLPESMEGYTWIGSLKLGDYSYANFREIDLAKRYITSLYFAIVTMATVGYGDIHAVNIREMIFVMIYVSFDMILGAYLIGNMTALIV 329
Papaver_GORK IRINYLFTRIVKLLAVELYCTHTAACIFYYLATTLPAEKEGYTWIGSLKLGDYSYSNFREIDLGKRYIVSLYFAIVTMATVGYGEIHAVNVREMIFVMIYVSFDMILGAYLIGNMTALIV 331
Amborella_GORK IRINYLFTRIVKLIVVELYCTHTAACIFYYLATTVPESEEGYTWIGSLTMGDYSYSHFREIDFIKRYLTSLYFAIVTMATVGYGDIHAVNPREMIFIMIFVSFDMILGAYLIGNMTALIV 314
Vulgaris_GORK IRINYLFTRIVKLLTVELYCTHTAACIFYYLATTLPEREEGYTWIGSLTLGDYSYSHFREIDIWRRYTVSLYFAIVTMATVGYGDIHAVNMREMIFIMIYVSFDMVLGAYLIGNMTALIV 341
Chenopodium_GORK IRINYLFTRIVKLLTVELYCTHTAACIFYYLATTIPEREEGYTWIGSLTLGDYSYSHFREIDLWRRYTTSLYFAIVTMATVGYGDIHAVNMREMIFIMIYVSFDMILGAYLIGNMTALIV 339
Lactuca_GORK IRVNYLFSRIIKLIAVELYCTHTAACIFYYLATTLPAVEEGYTWIGSLKLGDYSYSNFREIDLWKRYTTSLYFAIVTMATVGYGEIHAVNMREMIFVMIYVSFDMVLGAYLIGNMTALIV 331
Daucus_GORK IRIKYLFCRIVKLIVVEIYCTHTAACIFYYLATTLPAEKEGYTWIGSLKLGDYSYSNFREIDLWTRYITSLYFAIVTMVTVGYGDIHAVNLREMVFIMIFVSFDMVIGAYLIGNMTALIV 337
Medicago_GORK IRVNYIIARIVKLLVVELYCTHTAACIFYYLATTLPESQEGYTWIGSLKLGDYAYSKFREIDIWKRYTTSLYFAIVTMATVGYGDIHAVNLREMIFIMIYVSFDMVLGAYLIGNMTALIV 336
Prosopis_GORK IRINYMFTRIVKLIVVELYCTHSAACIFYYLATTLPPSQEGYTWIGSLQLGGYSYMNFREIDLWKRYTTSLYFAIVTMATVGYGDIHAVNMREMIFIMIYVSFDMVLGAYLIGNMTALIV 344
Nicotiana_GORK IRINYLFTRIVKLITVELYCTHTAACIFYYLATTLSEQQEGYTWIGSLKLGDYSYSNFRDIDLWTRYTTSMYFAIVTMATVGYGDIHAVNLREMIFVMIYVSFDMILSAYLIGNMTALIV 319
Solanum_GORK IRINYLFTRIVKLITVELYCTHTAACIFYFLATTLSEQQEGYTWIGSLKLGDYSYSNFRDIDLWTRYTTSMYFAIVTMATVGYGDIHAVNLREMIFVMIYVSFDMILSAYLIGNMTALIV 327
Coffea_GORK IRINYLFTRIVKLIAVELYCTHTAACIFYYLATTLPPEKEGYTWIGSLKLGDYQYSSFRDIDLWKRYTTSMYFAIVTMATVGYGDIHAVNVREMIFIMIYVSFDMILGAYLIGNMTALIV 324
Sesamum_GORK IRINYLFTRIVKLIAVELYCTHTAACIFYYLATTLPEEKEGYTWIGSLKLGDYSYAHFREIDIWKRYTTSMYFAIVTMATVGYGDIHAVNLREMIFIMIYVSFDMILGAYLIGNMTALIV 338
Cucumis_GORK IRINYMFTRIVKLLVVELYCTHTAACIFYYLATTLPASEEGYTWIGSLKLGDYSYSHFREIDLWKRYTTSLYFAIVTMATVGYGDVHAVNLREMIFIMIYVSFDMVLGAYLIGNMTALIV 327
Vitis_GORK TRINYMFTRILKLIAVELYCTHTAACVFYYLATTLPQSEEGYTWIGSLKLGDYSYSHFREIDIWKRYTTSLYFAIITMATVGYGDIHAVNLREMIFVMIYVSFDMILGAYLIGNMTALIV 318
Cannabis_GORK IRINYIVTRIIKLIAVELYCTHTAACIFYYLATTLPPSKEGYTWIGSLKLGDYSYSSFRDIDLWKRYITSLYFAIVTMATVGYGDIHAVNMREMIFIMIYVSFDMILGAYLIGNMTALIV 338
Gossypium_GORK IRINYLFTRIIKLIFVELYCTHTAACIFYYLATTLPREKEGYTWIGSLKLGDYSYSSFREIDLWKRYTTSMYFAIVTMATVGYGDIHAVNMREMIFIMIYVSFDMVLGAYLIGNMTALIV 329
C-Linker/A′
C-linker/B′
C-linker/C′
C-linker/D′
Helix A
β1
β2
β3
Arabidopsis_GORK KGSNTERFRDKMNDLISFMNRKKLGRDLRSQITGHVRLQYDSHYTDTVMLQDIPASIRAKIAQLLYLPYIKKVPLFKGCSTEFINQIVIRLHEEYFLPGEVITEQGNVVDHLYFVCEGLL 431
Brassica_GORK KGSNTERFRDKMNDLASFMNRKKLRGDIRSQITHHVRLQYDSKFTNTVMLQDIPASIRAKIAQLLYTPYIEKIPLFKGCSSEFINQIVVRLHEEYFFPGEVITEQGNVVDHLYFVCEGSL 430
Zingiber_GORK KGSKTERFRDKMKDLLNYMNRNKLGKEIRDQIKGHVRLQYESNYTEASILQDIPISIRAKISQTLYRPYIERVPLFKGCSTEFVNQIVIRLQEEFFLPGEVLLEQGNAVDQLYFVCYGVL 455
Elaeis_GORK KGSKTERFRDRMKELIKYMNRNKLGKDIRDQIKGHVRLQYESSYTEASVLQDIPVSIRAKISQTLYKPYIENVPLFKGCSAEFIHQIIIKLQEEFFLPGEVILEQGNAVDQLYFVCHGKL 430
Phoenix_GORK KGSKTERFRDRMKDLVKYMNRNKLGKEIRDQIKSHVRLQYESSYTEASVLQDLPVSIRAKISETLYKPYIDNVPLFSGCSEEFIHQIIIKLQEEFFLPGEVLLEQGDAVDQLYFVCHGKL 429
Oryza_GORK KGSRTERFRDKMKEVIRYMNRNKLGKDIREQIKGHLRLQYESSYTEASVLQDIPVSIRAKISQTLYKPYIESIPLFKGCSAEFIQQIVIRLQEEFFLPGEVILEQGSAVDQLYFVCHGAL 464
Brachypodium_GORK KGSRTERFRDKMKEVIRYMNRNKLGKEIREQIKGHLRLQYESSYTEASVLQDIPISIRAKISQTLYKPYIESTPLFKGCSAEFIQQIVIRLQEEFFLPGEVILEQGSAVDQIYFVCHGEL 446
Panicum_GORK KGSRTERFRDKMKEVIRYMNRNKLGKEIREQIKGHLRLQYESSYTEASVLQDIPISIRAKISQTLYKPYVESVPLFKGCSAEFIQQIVIRLQEEFFLPGEVILEQGSAVDQLYFVCYGAL 449
Papaver_GORK KGSKTERFRDKMADIMKYMNRNKLGKEIRDQIKGHLRLQYESSYTEAVVLQDIPISIRAKISQTLYRDFIEDVPLFKGCSPELKNQIVIRLHEEFFLPGEVIMEQGNIVDQIYFVCDGVL 451
Amborella_GORK KGSKTERFRDKMTDLIKYMNRNKLEKEIRDQIKGHVRLQYESSYTEASVLQDIPVSIRAEISQSLYKSTIEAVPLLKGCSSEFINQIVIRLHEEFFLPGEVILEQGNAVDQIYFISHGVV 434
Vulgaris_GORK KGSKTERFRDKMTEVMKYMNRNRLSRELRSQIKGHLRLQYESSYTEASILKDIPISLRAKISQTLYTPYIGRGPLFKGCSSEFINQIVTRVHEEFFLPGEVILEQGNVVDQLYFVCHGLL 461
Chenopodium_GORK KGSKTERFRDKMTEVMKYMNRNRLSRDLRNQIKGHLRLQYESSYTEASVLQDIPISLRAKISQSLYMPYIEKVPLFKGCSPEFINQIAIRVHEEFFLPGEVILEQGNVVDQLYFICHGLL 459
Lactuca_GORK KGSKTERYRDRMTDLLKYMNRNRLGRDIRNQIKGHLRLQYESNYTDSTILRDLPISIRAKISQTLYKSYIEKVSLFKGCSLEFINQVVTKVHEEFFLPGEVIMEQGNAVEQLYFICHGEL 451
Daucus_GORK KGSKTERYRDKMTDIIKYMNRNRLGRDIRNQIKGHLRLQYESTYTDAAALQDLPISIRAKISQTLYMSCVENVSLFKGCSSEFISQIVTRVHEEFFLPGELIMEQGNVVDQLYIVCHGLL 457
Medicago_GORK KGSKTEKFRDRMTDLMKYMNRNKLHKDIREQIKGHVRLQFESSYTDAAVLQDIPISIRSKISESLYSPYIKNVSLFSGCSSEFINQIVTRLHEEFFLPGEVIMQQGYVVDQLYFVCDGVL 456
Prosopis_GORK KGSKTEKFRDRMADLLKYMNRNKLGRDIREQIKGHMRLQYESSYTEPAAIQDLPISIRSKISQDLYLPYIEKVPLFKTCSSEFINQIVTRLHEEFFLPGEVILEQGNVVDQLYFVCHGVL 464
Nicotiana_GORK KGSKTERYRDKMTDLLKYMNRNRLGRDIRNQIKGHLRLQYESAYTDAAVLQDIPISIRAKISQSLYQSYIENVPLFKGCSSEFISQVVTRVHEEFFLPGEVIMEQGNVVDQLYFVCHGVL 439
Solanum_GORK KGSKTERYRDKMTDLLKYMNRNRLGRDIRSQIKGHLRLQYESAYTDAAVLQDIPISIRAKISQNLYQSYIENVPLFKGCSLEFISQVVTRVHEEFFLPGEVIMEQGNVVDQLYFVCHGVL 447
Coffea_GORK KGSKTEKYRDKMTDLIKYMNRNRLGKDIRNQIRGHLRLQYESSYTDAAVLQDIPISIRAKISQSLYKSYIEEVILFKGCSAEFINQIVTRVHEEFFLPGEVIMEQGHAVDQLYFVCHGVL 444
Sesamum_GORK KGSKTERYRDKMTDLIKYMNRNRLGKNLRNQIKGHLRLQYESSYTDASVLQDIPISIRAKISQTLYKSYVENVPLFNGCSSEFINQIVTRVHEEFFLPGEVIMEQGNVVDQLYFVCHGVL 458
Cucumis_GORK KGSKTVKFRDKMADVMKYMNRNRLSREIRDQIKGHLRLQYESSYTEATVLQDIPISIRAKISQTLYLPYVQNVSLFRGCSPEFINQIVIRLHEEFFLPGEVIMEQGNVVDQLYFVCHGVL 447
Vitis_GORK KGSKTERFRDKMTDVIKYMNRNRLDRDVRNQIKGHLRLQYESGYTEASVIQDLPISIRAKIAQTLYKPLVEKVSLFRGCSLELINQIVIRVHEEFFLPGEVIMEQGNVVDQLYFVCHGML 438
Cannabis_GORK KGSKTEKFRDKMTDLIKYMNRNRLGKDIRNQIKGHVRLQYESSYTEASALQDIPISIRAKISQSLYLPFMEKVSLFRGCSSEFINQIVVKVHEEFFLPGEVIMEQGNVVDQLYFVCHGSL 458
Gossypium_GORK KGSKTEKFRDKMADVIKYMNRNKLDRDLRNQIKGHLRLQYESTYTEAAVLQDIPISIRAKISQSLYLPYIENASLFKECSSEFINQIVIRLHEEFFLPGEVIMEQGNVVDQLYFVCHGVL 449

```
                       β4          β5   β6  Helix P     β7       β8    Helix B       Helix C                                       ANK1
Arabidopsis GORK       EALVTKTDGSEESVTLLGPHTSFGDISIICNISQPFTVRVCELCHLLRLDKQSFSNILEIYFHDGRTILNNIMEEKE---SNDRIKKLESDIVIHIGKQEAELALKVNSAAFQGDFYQLK   548
Brassica_GORK          EALETKTDGTEDLVELLEPHTSFGDISIICNISQPFTIRVRSLCHLLRLDKQSFSNILEIYFHDGRKILNNLMEGKE---SNERIKKLESDIMIHIGKQEAELALKVNSAAFQGDIYQLK   547
Zingiber GORK          EGITIGEDGSEETLLLLEPNSSFGEISILCNIPQPYAVRVRELCRLLRLDKQLFANIMEIYFVDGRTILSNLIEEN-E--SNGRIKHLESDITFHIGKQEAALALQVNSAAYYGDLLQLK   572
Elaeis_GORK            EGVGIGEDGP----LELEPNSSFGEIAILCNIPQPFTVRVCELCRLLRIDKQIFTNILQIYFVDGRKILSNLLEGN-D---SIQIKQLEGDIIFHIGKQEAELALRVNNAAFYGDLHYLK   542
Phoenix GORK           EGVGIGEDGSKDTVLTLQPNSSFGEIAILCNIPQPFTVRVCELCRLLRIDKQVFTNILQIYFVDGRRILNNLLEGN-D---SNRIKQLESDITFHITKQEAELALRVNSDAFYGDLHHLK   545
Oryza_GORK             EGVGIGEDGQEETILMLEPESSFGEIAVLCNIPQPFTVRVCELCRLLRLDKQSFTNILEIFFVDGRRILSNLSESS-E--YGSRIKQLESDITFHIGKQEAELTLRVNNAAFYGDMHQLK   581
Brachypodium GORK      EGVGIGEDGQEETLLMLEPESSFGEIAILCNIPQPYSVRVCELCRLLRLDKQSFTNILEIYFVDGRKILSNLTENN-E--YGGRVKQLESDITFHIGKQEAELTLRVNSAAFYGDLHQLK   563
Panicum_GORK           EGVGIGEDGQEETLLMLEPESSFGEISILCNIPQPYTVRVCELCRLLRLDKQSFTNILEIYFVDGRRILSNLSE-S-E--YGGRVKQLESDITFHIGKQEAELILRVNSAAFYGDLHQLK   565
Papaver GORK           EEMGIGEEGSEVTVSLLEPNSSFGELSILCNMPQPYTIRVCELCRLLRLDKESFISILEICSSDERIILTNLLEGKESNKDFHRMKQLESDVMFHIGKQEGELALRVNSAACHGDLYHLK   571
Amborella_GORK         EEVGIGEDGLEETIVQLEHDNSFGEIAILCNIPQPYTVRVCELCRLLRLDKQSFSNILQIYFIDARTVLNNLLEGK-E--SSLRLKQLESDIIFHINKQEAELALRVNSAAYYGDLYHLK   551
Vulgaris GORK          EEVGIGQDGSEETVSRLEPGSTFGQISIFCNIPQPTTVRVLELCRLLRIDKESLSNIIDIYFYDGKKIFDNLLEGN-D--GKYNLKQVESDIASHIGKQESELALKVNNAAYHGDLYQIK   578
Chenopodium_GORK       EEVGIGQDGSEQIISRLEPNNTFGQISIFCNVPQPSIIRVIDLCRLLRIDKESLSNIIDIYFYDGKKIFDNLLEGNNN--GKYNLKQVESDIASHIAKQESELALRVNNAAHHGDLYQLK   577
Lactuca GORK           EEIGICEDGSEETVSILKPHSSFGEVSILCNIPQPYTVRVCELCRLLRLDKQSFSNILEIYFHDGRKILNNLVEFN-A--SDARMKQLETDIILHIGKHEAELALRVNSSAFYGDLYQLK   568
Daucus_GORK            EEVGICEDGTEETVSVLRPHSLFGEVSILCNIPQPYTVKVSELCRLLRLDKQSFSNILEIYFHDGRKILNNLLEGK-E--SNLRLKQLESDITFHINKQEAELALRVNSAAYYGDLYQLK   574
Medicago GORK          EEVGIADDGSEETVALLERNSSFGEISILCNIPQPHTVRVCELCRVLRIDKQSFSNILDIYFYDGKKVLDNLLEGK-E--S-IRGKQLESDITFHIGKLESELALKVNRTAFDGDLYQLK   572
Prosopis_GORK          EEVGPGENGSEETVSLLEPNSSFGQISILCNIPQPYTVRVCELCRLLRLDKQSFTDILDIYFYDGRKVLNNLLEGK-D--S-SRGKQLESDITFHIGKQEAELALKVNNAAFNGDLNHIK   580
Nicotiana GORK         EEVGIAKDGSEETVALLEPNSSFGDISIVCNIPQPYTVRVCELCRLIRIDKQSFSNILEIYFHDGRRILSNLLQGK-E--SNLRVKQLESDIAFHIGKHEAELALKVNSAAYHGDLHQLK   556
Solanum_GORK           EEVGIAKDGLEETVSLLEPNSSFGDISIVCNIPQPYTVRVCELCRLLRIDKQSFANILEIYFHDGRRILSNLLQGK-E--SNLRVKQLESDIALHIGKHEAELALKVNSAAYHGDLHQLK   564
Coffea GORK            EEVGTAKDGSEETLSLLEPNSVFGIVSILCNIPQPYTVRVCELCRLLRIDKQSFSNILEVYFHDGRTVLTNLLEEK-D--SAFSLKQLESDITLHIVKQEAELALKVNSAAYYGDLQQLK   561
Sesamum GORK           EEVGIAADGSEDTVSLLEPNSLFGEISILCNIPQPYTVRVCELCRLLRIDKQSFSNILEIYFHDGRKVLTNLLEVI-T--D-----STISDITFHIGKQEAELALRVNSAAYYGDLYQLK   570
Cucumis GORK           EELGIGQDSSEETIDLLQPNSSFGEISILCNIPQPYTVRVCELCRLLRIDKQSFTNILDIYFYDGRKILNNLLEGK-E--TNLRVKQLESDITFHIGKQEAELALRVNSAAYHGDLYQLK   564
Vitis_GORK             EEIGIGADGSEETVLPLQPNSSFGEISILCNIPQPYTVRVLELCRLLRIDKQSFTDILEIYFYDGRRILNNLLEGK-E--SNLRVKQLESDITFHIGRQEAELALRVNSASYHGDLYQLK   555
Cannabis GORK          EEVGIGEDGSEETVSLLQPSSSFGEISILCNIPQPYTVRVCELCRLLRIDKQSFTNILDIFFYDGRKILNNLLEVK-E--SNLRVKQLESDITFHIGKQEAELALKVNSSAFHGDLHQLK   575
Gossypium_GORK         EGIAIGEDGSEETVSLLEPNSSFGEISILCNIPQPYTVRVCELCRLLRIDKQSFSNILEIYFYDGRKVLNNLLEGK-E--SNLRVKQLESDISFHIGRQEAELALRVNCAAYNGDFYQLK   566
                       * :    :.      *   . ** :::.**: **  ::* .**:::*:**: : .*:::   * : :: *: :                      *:  ** : *. * *:**  :  **:  :*

                                    ANK2                              ANK3                          ANK4
Arabidopsis_GORK       SLIRSGADPNKTDYDGRSPLHLAACRGYEDITLFLIQEGVDVNLKDKFGHTPLFEAVKAGQEGVIGLLVKEGASFNLEDSGNFLCTTVAKGDSDFLKRLLSSGMNPNSEDYDHRTPLHVA   668
Brassica_GORK          SLVRSGADPNKTDYDGRAPLHLAASRGYEDITLFLIQEGVDINQKDKFGNTPLLEAVKAGQDRVIDLLVKEGASFDLEDAGNFLCTVVVKGDSDFLKRLLSSGMDPNTEDYDHRTPLHVA   667
Zingiber_GORK          GLVKAGADPNKTDYDGRSPLHLAASRGFEDITSFLIQECVDINVSDNFGNTPLFEAVKNGHDKVASLLYNNGAKLNLKDPSSHLCSAVARGDSDFIKRLLAYGIDLNLKDYDSRTPLHVA   692
Elaeis_GORK            GLIQAGADPNKTDYDGRSPLHLAAAKGHEDITLFLIQEGVNINLSDNFGNTPLFEAVKVGHDRVASLLFSRGAQLNLKDAGSHLCTAAAKGDSDFIRRALSYGVDPNSKDYDHRTALHIA   662
Phoenix_GORK           GLIQAGADPNKTDYDGRSPLHLAAARGHEDITLFLIQEGVDINLSDNFGNTPLFEAIKDGHDRVASLLFSRGAQLSLKDAGSQLCAAAAEGDSDFIKRALSYGVDPNSKDYDHRTALHIA   665
Oryza_GORK             SLIRAGADPKNTDYDGRSPLHLAACKGFEDVVQFLLHEGVDIDLSDKFGNTPLLEAVKQGHDRVATLLFSKGAKLSLENAGSHLCTAVARGDTDFVRRALAYGGDPNARDYDHRAPLHIA   701
Brachypodium_GORK      GLIRAGADPKNTDYDGRSPLHLAASKGYEDVAQFLIHEGADINLIDKFGNTPLLEAVKQGHDRVATLLFKKGAILNLQNAGSHLCSAVSKGDSDFIRRALACGADPDSKDYDHRSPLHIA   683
Panicum_GORK           SLIRAGADPKNTDYDGRTPLHLAACRGYEDVVQFLLAEGVDINLTDQFGNTPLLEAVKQGHERVAALLFAKGAKLSLKNAGSHLCTAVAKGDSDFIRRALAFGADPNCGDYDHRTPLHIA   685
Papaver_GORK           RLIRAGADPNKTDYDGRTPLHIAASEGFEHIASFLIQEGVGVNIADKFGNTPLFEAVKRGNDRVASLLVKEGASLNIVDGGSCLCQAVSRGDSDFVKRLLSNGLDPNSKDYDQRTALHVS   691
Amborella_GORK         GLIRAGADPKKTDYDGRSALHLAASKGFEDITTFLIRETVDVNLTDKFGNTPLLEAIRYGHDRVASLLVKEGASLDIDDAGGFLCKAVASGNTDFLKRLLVYGMDPNSRDYDYRTALHKA   671
Vulgaris_GORK          NLLNAGADMNKTDYNGRSPLHIAAARGCEEIILLVKEGVRINEKDNFGNTPLLEAVKNGNDKAAALLYREGARLDVKDVGSFLCTAVLGGDVDYLRRILANGIDPNSKDYDYRTPLHVA   698
Chenopodium_GORK       SLLNAGADLKKTDYNGRTPLHIAASGGCEDIVLFLIEEGADVNRTDNFGNTPLLEAVKNGHDKVAALLYKEKARIDVKDVGSFLCTVVLSGDVEFLKRILTNGMDPNSKDYDHRTPLHVA   697
Lactuca_GORK           SLIRAGADPNKKDYDGRTPLHLAASKGYEDITLFLIQEKVEVNVLDNFGNTPLLEAIKNGHDKVASILVKEGGSLKIDDAGWFLCTSVARGDIDYIRRILSNGVDPNSKDYDFRTPLHVA   688
Daucus_GORK            GLVRAGADPNKTDYDGRSPLHLAASKGYEDIILFLTQEGVDINISDNFGNTPLFEAIKSGHDQVVSLLIKEGAILKIGDSGPFLCTAVARGDYDLIKRVLSAGIDPNSSDYDHRTPLHVA   694
Medicago_GORK          SLIRAGADPKKTDYDGRSPLHLAACRGYEDITLLLIHERVDMNVKDNFGNTPLLEAVKNGHDRIASLLVREGASLKIDDGGSFLCSAVARGDSDYLKRLLSNGMDANLKDYDHRTPLHVA   692
Prosopis_GORK          GLIRAGADPNKADYDGRSALHLAASRGFEDITIFLVQEGVEIDLRDNFGNTPLLEAVKNGHDRVASLLVGKGASMKIEDAGSVLCNAVARGDSDYLKRLLSYGMDPNTKDYDYRSPLHVA   700
Nicotiana_GORK         SLIRAGADPNKKDYDGRSPLHLAASRGYEDITLFLIQEGVDINAPDKFGNTPLLEAIKSGHDRVASLLVKEGAFLKIENAGSFLCMVIAKGDSDLLRRLLSNGVDPNSKDYDQRTPLHVA   676
Solanum_GORK           SLIRAGADPKKKDYDGRSPLHLAASRGYEDITLFLIQEGIDINAPDKFGNTPLLEAIKIGHDRVASLLVKEGALLNIENAGSFLCMVIARGDSDLLRRLLSNGVDPNTKDYDQRTPLHVA   684
Coffea_GORK            NLIRAGADPNKNDYDGRSPLHLAASRGYEDIAQFLIQEGVDINVTDNFGNTPLLEAIKSGHEHVASLLVKEGASLQIENAGNFLCTVVAKGDSDLLRRFLTRGIDPNSKDYDQRTPLHVA   681
Sesamum_GORK           SLIRSGADPNKKDYDGRSALHLAASRGYEDVTLFLIQEGVDINAEDNFGNTPLLEAIKSGHDRVASLLSREGALLKIDNPGAYLCTVVSKGDTDLLRRVLANGIDPNSKDYDHRTPLHLA   690
Cucumis_GORK           GLVRAGADPNKTDYDGRSPLHLAASRGFEDIVVFLIQEGVNIDLKDNFGNTPLMEAIKNGNDQVAVLLSKEGASLKVDNPGSFLCTAVSRGDSDLVKRLLCYGIDPNSKDYDSRTPLHIA   684
Vitis_GORK             SLIRAGADPNKTDYDGRSPLHLASARGFEDIVTFLIQEGVDVNISDNFGNTPLLEAIKNAHDRVASLLVNKGALLKIDDAGGFLCATIARGDSDFLKRILSNGIDPNSKDYDHRTPLHVA   675
Cannabis_GORK          SLIRAGADLNKTDYDGRSPLHLAASRGYEDITRFLIQQGVNVNAIDNFGNTPLLEALKNGHDRVSSLLVQEGASLMIDNAGSFLCTAVSRGDSDFLKRVLSNGVDPNSKDYDHRSPLHVA   695
Gossypium_GORK         SLIRAGADLNKTDYDGRSPLHLAASKGYEDITSFLIRHPVDINLKDKFGNTPLLEALKNGHDNLAALLIKEGASLNIDDAGSYLCTAVAKGDSDFLRRLLSNGVDPNSRDYDHRTPLHVA   686
                         *:.:*** :: **:**: **:*:. * *.:  :*  .   ::  *:**:***:**:: .::    :*  . . : : : .  **     *: : ::* *  * : :  *** *: ** :
```

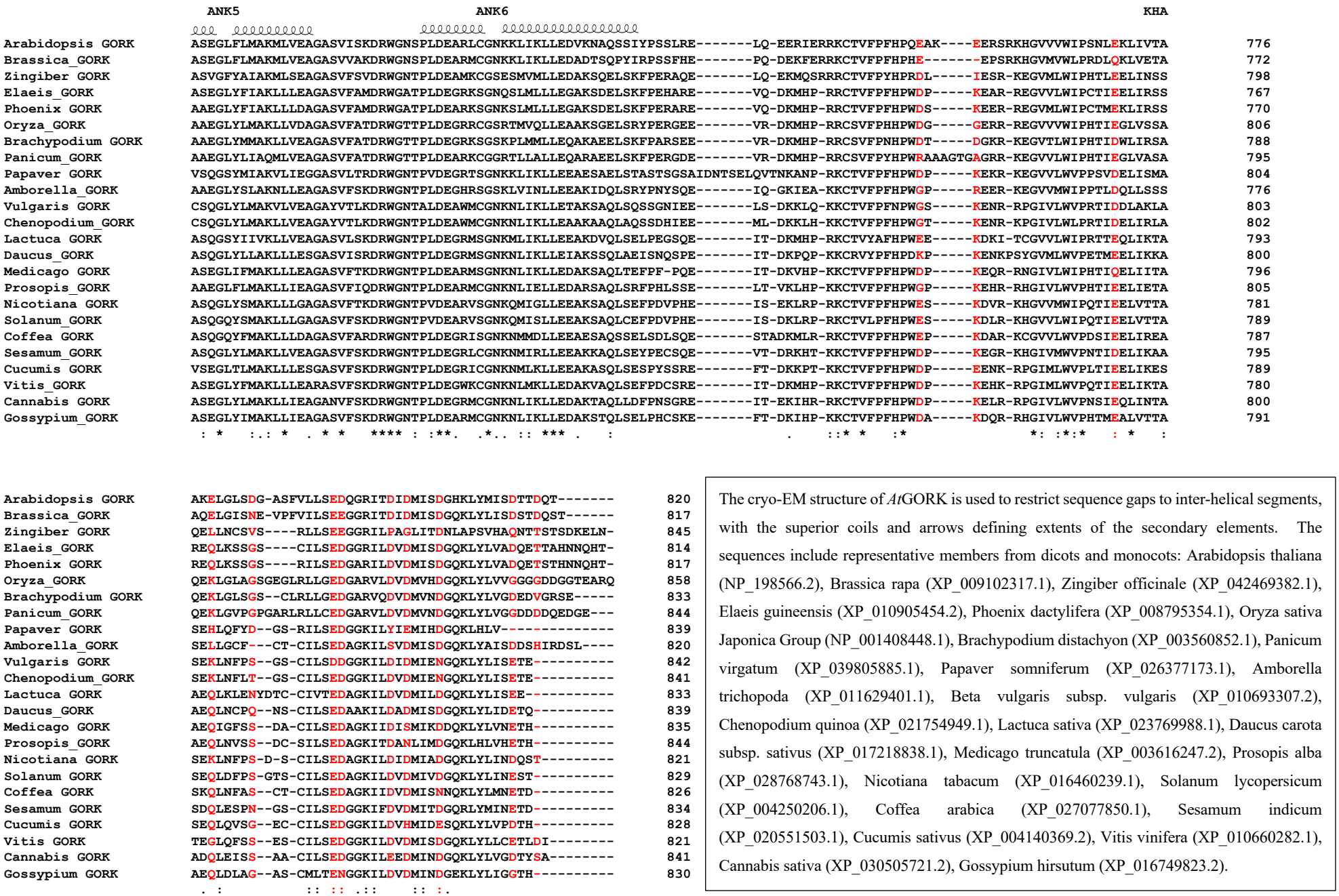

The cryo-EM structure of *At*GORK is used to restrict sequence gaps to inter-helical segments, with the superior coils and arrows defining extents of the secondary elements. The sequences include representative members from dicots and monocots: Arabidopsis thaliana (NP_198566.2), Brassica rapa (XP_009102317.1), Zingiber officinale (XP_042469382.1), Elaeis guineensis (XP_010905454.2), Phoenix dactylifera (XP_008795354.1), Oryza sativa Japonica Group (NP_001408448.1), Brachypodium distachyon (XP_003560852.1), Panicum virgatum (XP_039805885.1), Papaver somniferum (XP_026377173.1), Amborella trichopoda (XP_011629401.1), Beta vulgaris subsp. vulgaris (XP_010693307.2), Chenopodium quinoa (XP_021754949.1), Lactuca sativa (XP_023769988.1), Daucus carota subsp. sativus (XP_017218838.1), Medicago truncatula (XP_003616247.2), Prosopis alba (XP_028768743.1), Nicotiana tabacum (XP_016460239.1), Solanum lycopersicum (XP_004250206.1), Coffea arabica (XP_027077850.1), Sesamum indicum (XP_020551503.1), Cucumis sativus (XP_004140369.2), Vitis vinifera (XP_010660282.1), Cannabis sativa (XP_030505721.2), Gossypium hirsutum (XP_016749823.2).

Figure S3. Sequence alignments for the representative GORKs from both dicots and monocots.

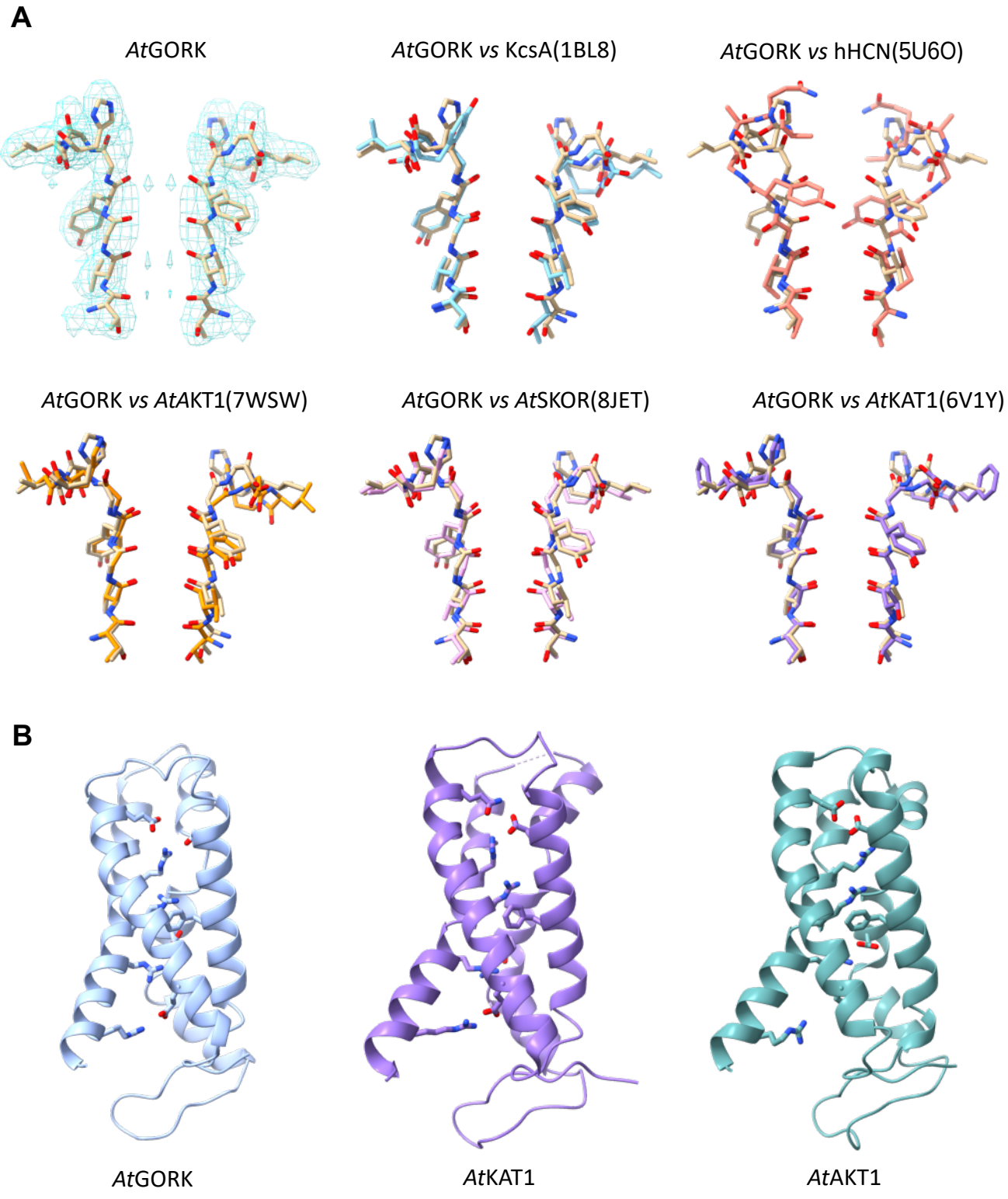

Figure S4. Structural comparison of K^+-selectivity filter and VSD of *At*GORK with other K^+ channels.

(**A**) Comparison of K^+-selectivity filters from *At*GORK with other K^+ channels. (**B**) Comparisons of voltage sensing domain (S1-S4) from *At*GORK (light-blue), *At*KAT1(purple, 6V1Y) and *At*AKT1 (dark-green, 8WSW). The S4 helix in these three K^+ chan nelcontains conserved positively charged residues, as shown in sticks, and adopt a resting "up" conformation.

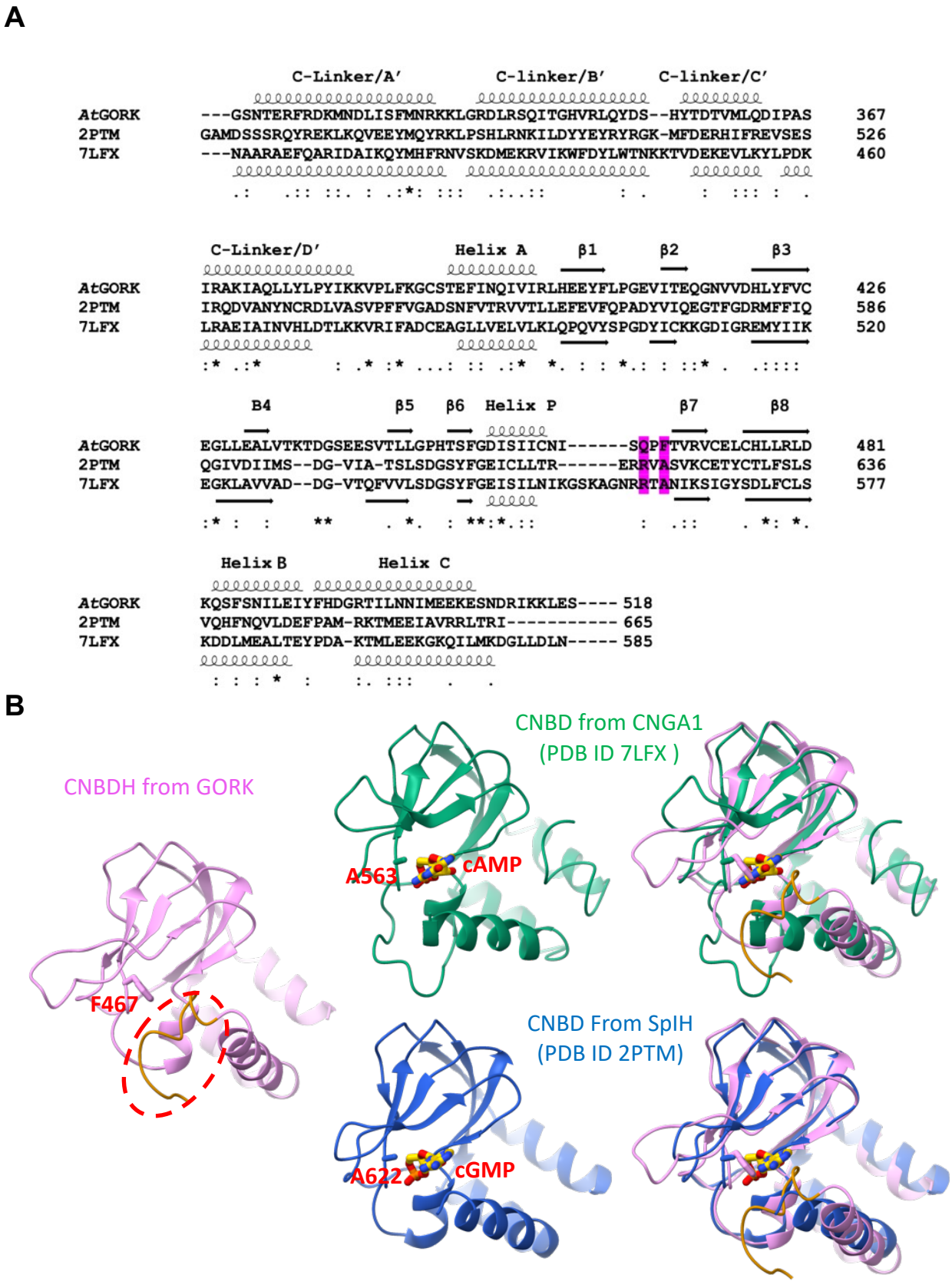

Figure S5. Structural comparison of CNBD domain of *At*GORK with other K^+ channels.

(**A**) Structure-based sequence alignment of CNBDH of *At*GORK with CNBD from other K^+ channels. (**B**) Comparisons of CNBDH of *At*GORK with CNBDs from CNGA1 (7LFX, green) and SpIH (2PTM, blue). A small side-chain residue alanine (A 563in 7LFX, or A622 in 2PTM), located at the entrance of the cAMP/cGMP binding pocket, is replaced by bulky phenylalanin e (F467in *At*GORK), which likely blocks access for the secondary messenger molecules. Helix C adopts a closed conformation, with itsadjacent connecting loop (red circle) to the next domain positioned at the entrance of the cAMP/cGMP binding site, in dicatingthat large conformational changes would be required for cAMP/cGMP binding.

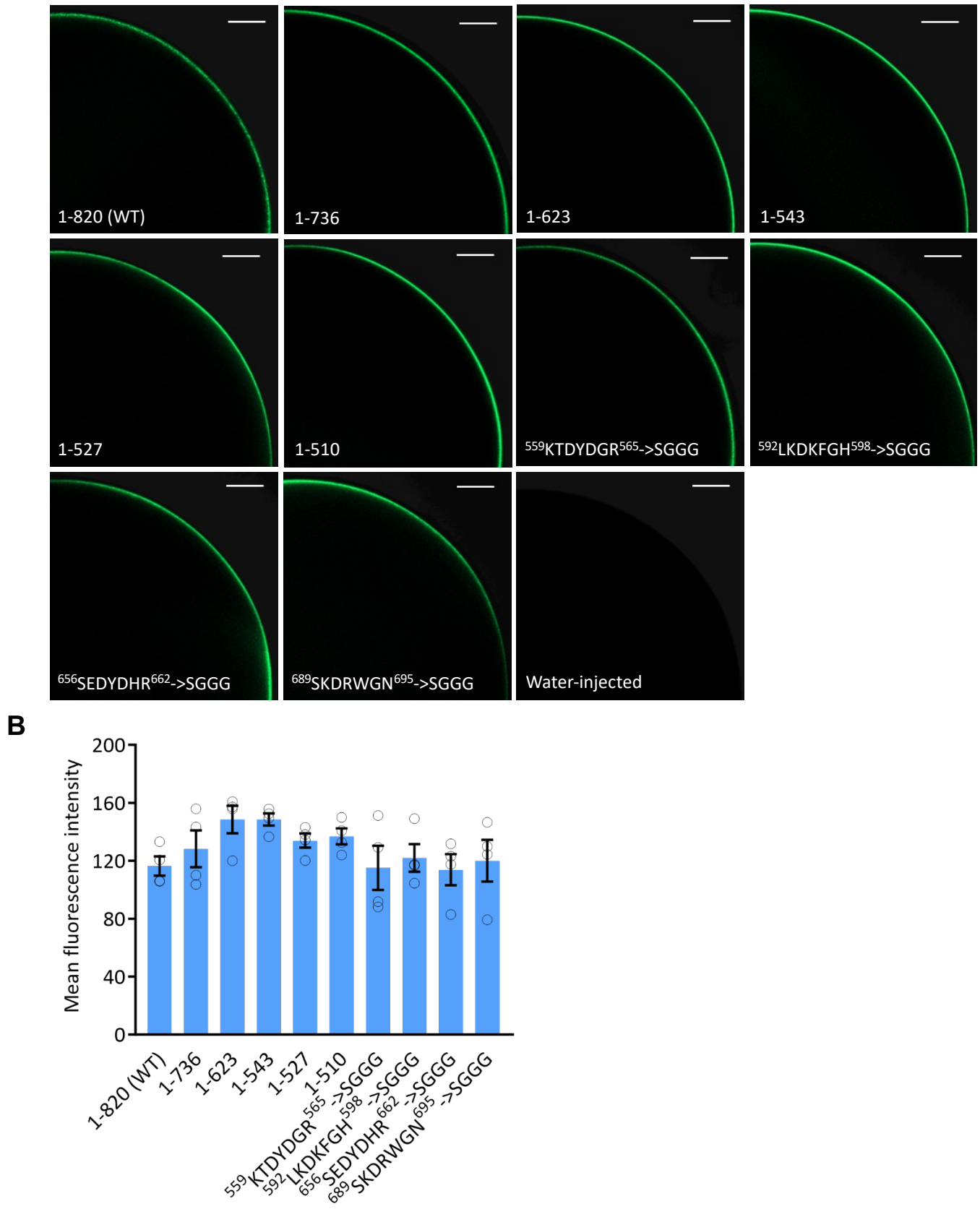

Figure S6. Fluorescence and confocal imaging of the N-terminal GFP tagged *At*GORK.

(**A**) Representative fluorescence images of *At*GORK wild-type (1-820) and mutants corresponding to Figure 3. The GFP fluorescence on the plasma membrane of oocytes was analyzed by LSM980 laser confocal microscope. The quarter of the whole cell is shown. Scale bars: 100 μm. (**B**) Mean fluorescence intensity measurements in ImageJ. A one-way ANOVA analysis was performed with a *P* value of 0.1298. Data are mean ± SEM, $n = 4$.

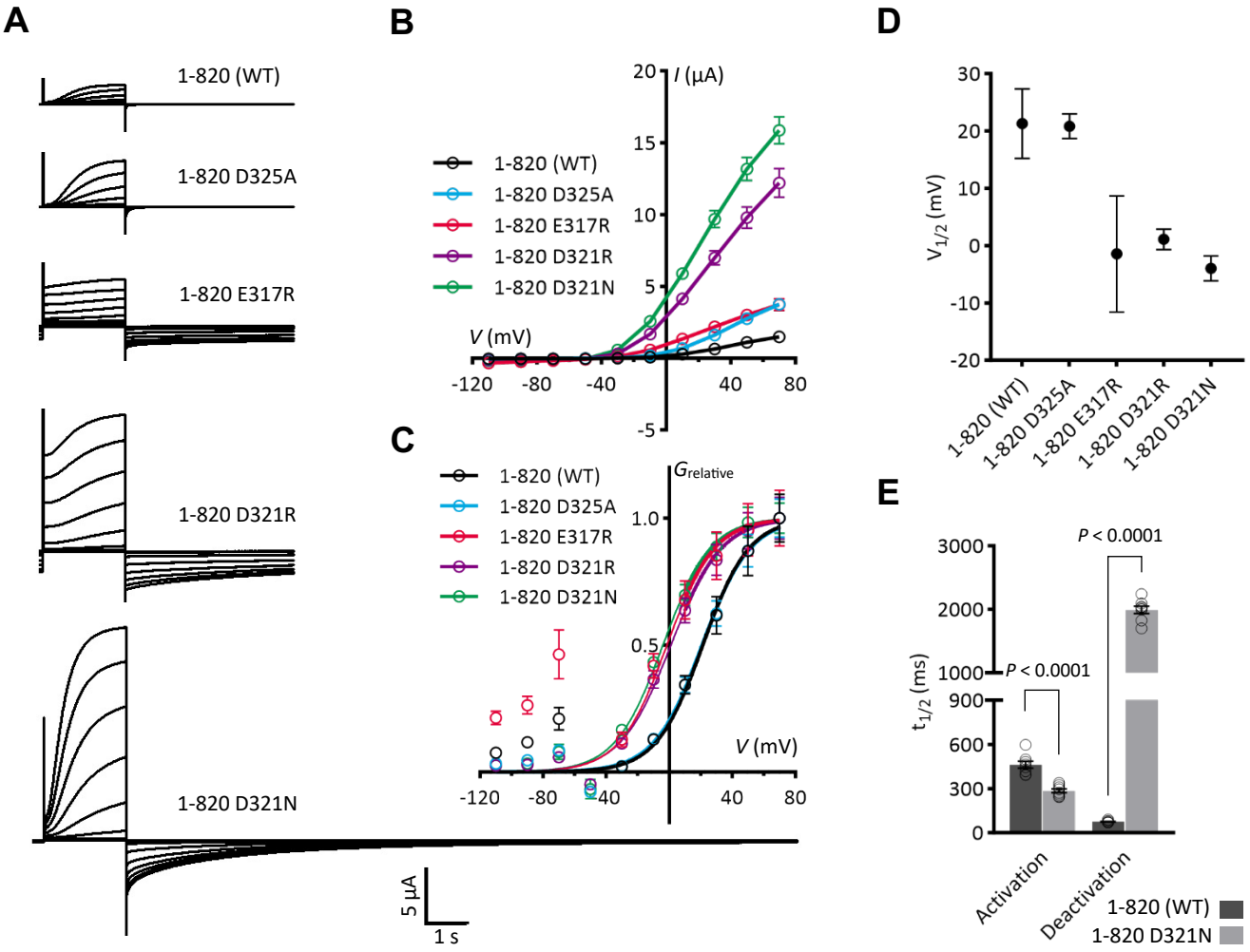

Figure S7. Mutational tests of conserved acidic residues at the C-linker/TMD interface in full-length *At*GORK.

(**A**-**E**) Electrophysiological analyses of E317, D321 and D325 mutations in *At*GORK$^{1\text{-}820}$. Representative current traces (**A**) and steady-state current-voltage (*I*-*V*) relations (**B**) are shown. Relative conductance-voltage ($G_{relative}$-*V*) curves (**C**) and half-activation voltage ($V_{1/2}$) values (**D**) were generated through Boltzmann sigmoidal fitting (outliers excluded). Conductance was calculated using the equation $G = I/(V - E_K)$, where *I* is the steady-state current, *V* is the test potential, and E_K (–58 mV) was derived from the Nernst equation based on intracellular (~100 mM) and extracellular (10 mM) K^+ concentration in the oocyte TEVC recordings. Relative conductance was calculated by normalization to the maximal conductance. Halftime ($t_{1/2}$) for activation at +70 mV and deactivation at −110 mV, calculated as $\ln(2)\cdot\tau$ where τ is the time constant from single-exponential decay fitting, is shown in (**E**). Data are mean ± SEM, $n \geq 8$. Significance analysis was performed using unpaired Student's t-test, with *P*-values displayed on the bar charts.

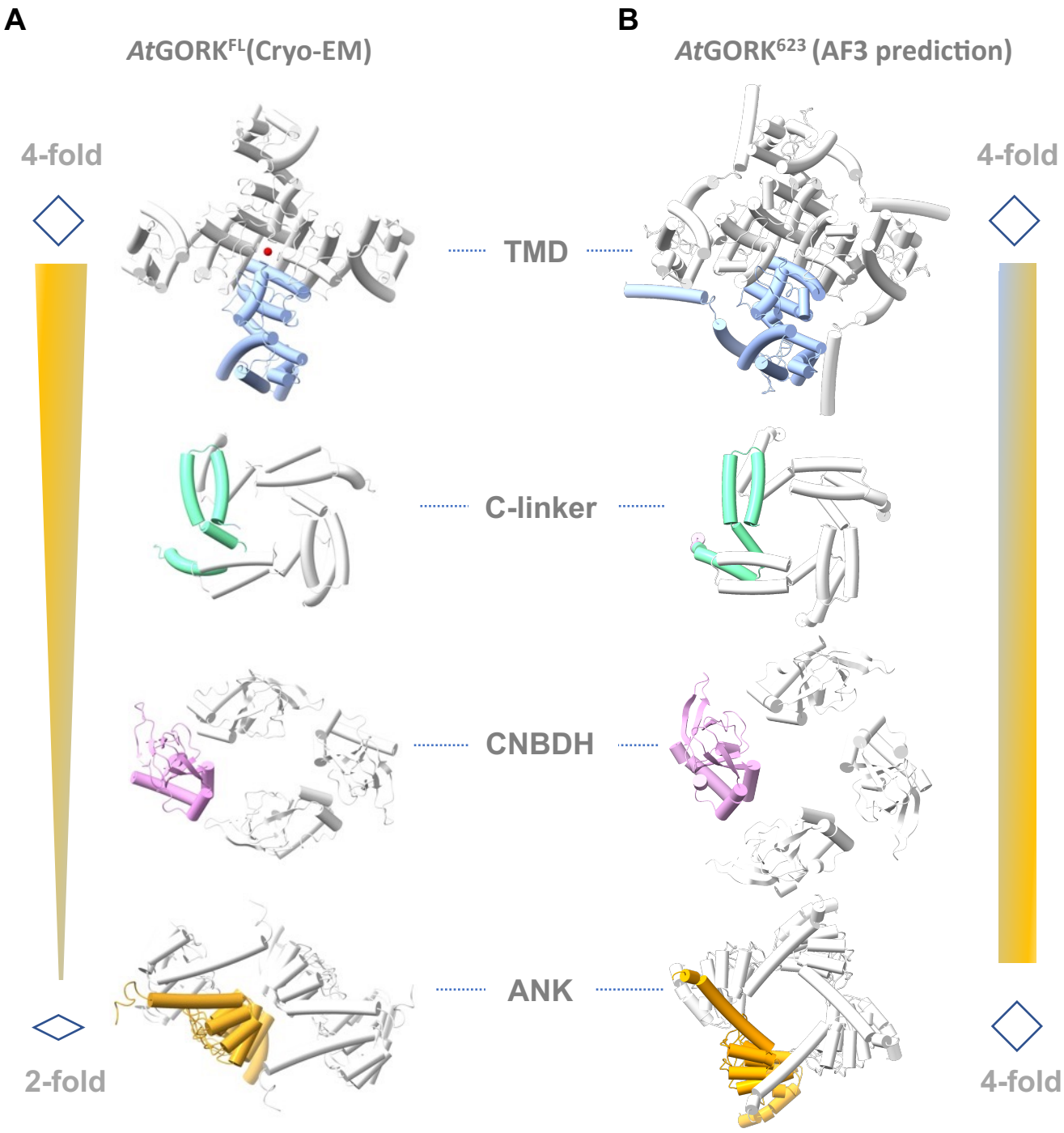

Figure S8. Symmetry analysis of domain assembly in *At*GORK^{FL}(Cryo-EM) and *At*GORK^{623}(AF3 prediction).

Table S1: Statistics of data collection, image processing, and model building

Sample	AtGORK^{FL1}	AtGORK^{FL2}	AtGORK^{623}	AtGORK^{510}
PDB	9KHF	8WFZ	9KHE	9KHG
EMDB	62338	37500	62337	62339
		Data collection and processing		
Microscope	Titan Krios	Titan Krios	Titan Krios	Titan Krios
Detector	Gatan K3	Gatan K3	Gatan K2	Gatan K3
Magnification	22,500 ×	22,500 ×	130,000 ×	22,500 ×
Voltage (kV)	300	300	300	300
Electron exposure (e-/Å^2)	50	50	50	50
Nominal defocus range (μm)	-1.2 to -2.0	-1.2 to -2.0	-1.2 to -2.0	-1.2 to -2.0
Frames per movie	32	32	32	32
Pixel size (Å)	1.06	1.06	1.04	1.06
		Reconstruction		
Software	cryoSPARC 3.2	cryoSPARC 3.2 & Relion 3.0	cryoSPARC 3.2	cryoSPARC 3.2
Symmetry imposed	C2	C1	C4	C4
Initial particle images (no.)	18,650,563	18,650,563	1,139,470	2,840,921
Final particle images (no.)	156,313	39,551	75,626	141,755
Map resolution (Å)	3.4	4.3	3.2	3.3
		Refinement and model validation		
CC (mask)	0.7	0.76	0.82	0.84
CC (box)	0.63	0.66	0.58	0.64
CC (peaks)	0.55	0.45	0.54	0.62
CC (volume)	0.66	0.76	0.81	0.80
RMSD Bond Length (Å)	0.003	0.003	0.003	0.003
RMSD Bond angles (degrees)	0.632	0.701	0.627	0.572
Favored (%)	94.96	96.52	95.47	97.83
Allowed (%)	4.85	3.48	4.53	2.17
Ramachandran plot outliers (%)	0.19	0.00	0.00	0.00
Molprobity score	2.01	1.97	1.91	1.57
Clash score	14.33	17.44	11.95	10.17

Reference

Deng, Y.N., Kashtoh, H., Wang, Q., Zhen, G.X., Li, Q.Y., Tang, L.H., Gao, H.L., Zhang, C.R., Qin, L., Su, M.*, et al.* Structure and activity of SLAC1 channels for stomatal signaling in leaves. Proc Natl Acad Sci U S A 2021;**118**.

Emsley, P., Lohkamp, B., Scott, W.G., and Cowtan, K. Features and development of Coot. Acta Crystallogr D Biol Crystallogr 2010;**66**:486-501.

Liebschner, D., Afonine, P.V., Baker, M.L., Bunkóczi, G., Chen, V.B., Croll, T.I., Hintze, B., Hung, L.W., Jain, S., McCoy, A.J.*, et al.* Macromolecular structure determination using X-rays, neutrons and electrons: recent developments in Phenix. Acta Crystallogr D Struct Biol 2019;**75**:861-877.

Mastronarde, D.N. Automated electron microscope tomography using robust prediction of specimen movements. J Struct Biol 2005;**152**:36-51.

Pettersen, E.F., Goddard, T.D., Huang, C.C., Couch, G.S., Greenblatt, D.M., Meng, E.C., and Ferrin, T.E. UCSF Chimera--a visualization system for exploratory research and analysis. J Comput Chem 2004;**25**:1605-1612.

Pettersen, E.F., Goddard, T.D., Huang, C.C., Meng, E.C., Couch, G.S., Croll, T.I., Morris, J.H., and Ferrin, T.E. UCSF ChimeraX: Structure visualization for researchers, educators, and developers. Protein Sci 2021;**30**:70-82.

Punjani, A., Rubinstein, J.L., Fleet, D.J., and Brubaker, M.A. cryoSPARC: algorithms for rapid unsupervised cryo-EM structure determination. Nat Methods 2017;**14**:290-296.

Wu, C., Huang, X., Cheng, J., Zhu, D., and Zhang, X. High-quality, high-throughput cryo-electron microscopy data collection via beam tilt and astigmatism-free beam-image shift. J Struct Biol 2019;**208**:107396.

Zivanov, J., Nakane, T., Forsberg, B.O., Kimanius, D., Hagen, W.J., Lindahl, E., and Scheres, S.H. New tools for automated high-resolution cryo-EM structure determination in RELION-3. Elife 2018;**7**.